Pre-transition softening and anomalous pressure dependence of shear constants in alkali and alkaline-earth metals due to band-structure effects

1991 J. Phys.: Condens. Matter 3 1409

(http://iopscience.iop.org/0953-8984/3/11/004)

J. Phys.: Condens. Matter 3 (1991) 1409–1428. Printed in the UK

Pre-transition softening and anomalous pressure dependence of shear constants in alkali and alkaline-earth metals due to band-structure effects

V G Vaks†, M I Katsnelson‡, A I Likhtenstein§, G V Peschanskikh‡ and A V Trefilov†

† I V Kurchatov Institute of Atomic Energy, Moscow 123182, USSR
‡ Institute of Physics of Metals, Sverdlovsk 620219, USSR
§ Institute of Chemistry, Sverdlovsk 620219, USSR

Received 5 March 1990, in final form 9 August 1990

Abstract. Band-structure and shear-constant ($C_{ss'}$) calculations have been performed for the Li, Na and Ba BCC phase and the Cs, Ca and Sr BCC and FCC phases within a broad range of compressions (U) from 0 to 40–55%. To describe the 'band' contributions to $C_{ss'}$, use is made of calculations based on the linear muffin-tin orbital/atomic sphere approximation (LMTO-ASA) method; the other contributions to $C_{ss'}$ are described by using the semiempirical 'electrostatic' model. At $U = 0$ the calculated $C_{ss'}$ values are usually close to the observed ones. We have revealed pronounced effects of softening for the shear constants, up to the loss of stability ($C_{ss'} < 0$), when the Fermi level approaches the maximum points of the density of states $n(\varepsilon)$, as well as under certain changes of shape of $n(\varepsilon)$. The compression values, at which this softening takes place, are in good agreement with the position of structural phase transitions under pressure, observed in the metals considered. A number of anomalies in the $C'(U)$ and $C_{44}(U)$ dependences are predicted, in particular a sharp drop of $C'(U)$ near the phase transition points $U = U_c$ in BCC Li and Ba and FCC Cs, Ca and Sr, as well as a significant decrease of $C_{44}(U)$ with rising U in FCC Cs and BCC Sr at $U \gtrsim 0.5$.

1. Introduction

The shear constants $C_{ss'}$ are an important characteristic of mechanical and strength properties of metals. Effects of band-structure variation on these constants, in particular those connected with the Fermi level proximity to the singular points in the density of states $n(\varepsilon)$, attract much attention. There are a number of experimental indications of clear manifestations of these effects in shear constants, e.g. the known anomalies of concentration and temperature dependences of $C_{ss'}$ in the BCC transition metals, which are assigned to the band effects by many authors [1–3]. The 'pre-martensitic anomalies', the appreciable softening of $C_{ss'}$ in a number of metals and alloys on approaching the points of structural phase transitions in the pressure or concentration, are also widely discussed [4–9]. As will be considered below, evidently this pre-martensitic softening is also usually attributed to the band effects.

The development of first-principles methods for band-structure and total-energy (E) calculations [10–12] made it possible to evaluate consistently and effectively the bulk

0953-8984/91/111409 + 20 $03.50

characteristics of metals, such as the pressure p and bulk modulus B. At the same time, the quantitative calculations of the shear moduli need much more computational efforts and are rather scarce as yet [13–16]. Therefore, the mentioned problems of band-structure influence on $C_{ss'}$ in metals has mainly been discussed qualitatively, using various model approximations [1–3, 17, 18]. Usually, the authors proceed from the relations

$$C_{ss'} = (1/N\Omega)\,\partial^2 E/\partial u_s\,\partial u_{s'} \tag{1a}$$

$$E = E_b + E_{es} \qquad C_{ss'} = C^b_{ss'} + C^{es}_{ss'} \tag{1b}$$

where N is the total number of atoms; Ω is the atomic volume; u_s is the shear deformation; E_b is the 'band' energy, equal to the sum of one-electron energies ε_λ over the occupied states; E_{es} (called for brevity the electrostatic energy) is the difference between E_{Mad}, the Madelung energy of ions, and U_{ee}, the terms electron–electron interaction double-counted in E_b; while $C^b_{ss'}$ and $C^{es}_{ss'}$ correspond to the substitution of $E = E_b$ and $E = E_{es}$, respectively, into equation (1*a*). Further, it is assumed that the 'band' anomalies in $C_{ss'}$ under discussion are determined mainly by the band contribution $C^b_{ss'}$, while in $C^{es}_{ss'}$ these anomalies are insignificant. Thus Ohta and Shimizu [3] did not consider $C^{es}_{ss'}$ at all and calculated only the $C^b_{ss'}$ term (within the tight-binding and rigid-band model) while Ashkenazi *et al* [1, 2] approximated $C^{es}_{ss'}$ by a certain smooth function of the volume, $A_{ss'}f(\Omega)$, with a fitting coefficient $A_{ss'}$. The assumption of the insignificance of the band effects in $C^{es}_{ss'}$ seems plausible and, for some models, it may be justified formally [17, 18]. Dacorogna *et al* [19] made an attempt at a more formal substantiation of the $C^{es}_{ss'} = A_{ss'}f(\Omega)$ interpolation using the 'frozen muffin-tin potential' approximation (which does not change under the shear deformation) in calculating $C_{ss'}$ within the linear muffin-tin orbital (LMTO) method. However, this work has been based on approximations and not rigorous proofs, and in another calculation [15] the above form for the $C^{es}_{ss'}$ term has not been obtained.

The present work is aimed at a further and still more detailed investigation of the influence of band-structure singularities on the shear constants. We shall discuss these problems by using the study of the $C_{ss'}$ dependences on pressure p in alkali and alkaline-earth metals as an example. With rising p, in all these metals (except Na) phase transitions occur between the BCC and close-packed structures, which were studied by many authors, see e.g. [7, 20–22]. Some anomalies in the pressure dependence of the averaged shear modulus $G(p)$ in polycrystalline Ba, Sr and Li were observed [4–6]. However, they have not yet been discussed theoretically.

We study the dependences of $C_{ss'}$ on the compression $U = (\Omega_0 - \Omega)/\Omega_0$ (where Ω_0 is Ω at $p = 0$) in the BCC and FCC phases of Li, Na, Cs, Ca, Sr and Ba and consider the following general problems by using these examples:

(i) the presence of band-structure-driven anomalies in the $C_{ss'}(U)$ dependences for the given class of metals, where they are evidently manifested still more vividly than those in the BCC d metals discussed earlier;

(ii) the peculiarity of these anomalies in the case when the band-structure variation with changing external parameter (here, with pressure, while in an alloy it may also be concentration) corresponds not to the rigid-band model (considered in [1–3, 17, 18]) but to a significant change of form of $n(\varepsilon)$, in particular in the vicinity of the Fermi level ε_F; and

(iii) the connection of the band anomalies in $C_{ss'}$ with the structural phase transitions and the microscopic mechanism of the presence or absence of 'pre-martensitic softening' of the shear constants.

In the same way as in [1–3] on $C_{ss'}$ in the d metals, in this work we mainly investigate the qualitative effects. Therefore, in our calculations we make use of approximations analogous to those used earlier. We shall calculate the band contribution $C_{ss'}^{b}$ in equation (1*b*) by using the linear muffin-tin orbital/atomic sphere approximation (LMTO-ASA) method within the 'frozen-potential' approximation in the same way as in [15], while $C_{ss'}^{es}$ will be assumed proportional to the $C_{ss'}^{Mad}$ contribution to $C_{ss'}$ from the Madelung energy of point ions: $C_{ss'}^{es} = AC_{ss'}^{Mad}$. Thus, we shall demonstrate that for all the metals considered the choice of the same value of $A = 5/3$ usually results in a good agreement of the calculated $C_{ss'}$ with the experimental values at $U = 0$. We have failed to obtain a substantiation of such a universal interpolation for the $C_{ss'}^{es}$. However, the results and considerations presented below allow one to assume that these relatively simple calculations of $C_{ss'}^{b}$ by the LMTO-ASA method, combined with the above-mentioned interpolation for $C_{ss'}^{es}$, may be useful not only for qualitative studies of the $C_{ss'}$ dependences on external parameters but also for semiquantitative estimates of the magnitudes of $C_{ss'}$ themselves, at least for some classes of metals and alloys.

In section 2 we describe the method and approximations of the calculations. The change with compression U of the electronic density of states $n(\varepsilon)$ in the metals under consideration is discussed in section 3. In section 4 we present the results of the $C_{ss'}(U)$ calculations within a broad range of compressions U from $U = 0$ to $U = 0.40$–0.55. In the same way as in [3], we calculate $C_{ss'}$ not only for actual values of the valence Z (i.e. $Z = 1$ or $Z = 2$) but also for a whole interval of values of the effective valence N_v, the number of occupied states in the valence band. This makes it possible to discuss qualitatively (within the rigid-band model) the cases of alloys as well. The presented results illustrate the above-mentioned points (i)–(iii). They also allow us to make a number of predictions about a peculiar variation of $C_{ss'}$ with pressure in the considered metals. The main conclusions are summarized in section 5.

2. Method and approximations of calculations

For each value of the atomic volume Ω the electronic structure was calculated by using the self-consistent LMTO method within the ASA. Use was made of the basis of orthogonal muffin-tin (MT) orbitals with the effective two-centre Hamiltonian determining the crystal energy spectrum [23]:

$$H_{lm,l'm'} = C_l + \Delta_l^{1/2} \tilde{S}_{lm,l'm'}(k) \Delta_l^{1/2} \tag{2a}$$

$$\tilde{S}(k) = S(k)[1 - \gamma_l S(k)]^{-1}. \tag{2b}$$

Here C_l and Δ_l are potential parameters characterizing the centre and width of the non-hybridized l-band; $S(k)$ is the matrix of structural constants of the LMTO method and γ_l is the energy band distortion parameter [23]. The Hedin–Lundquist [24] expression was used for the exchange–correlation potential. The pressure $p(\Omega)$ (presented below in the upper part of figures 5–9) was calculated according to the Pettifor [25] formula. In Li, Na, Cs, Ca, Sr and Ba the values of 143.4, 254.5, 747.7, 293.2, 379.1 and 426.9 au were used, respectively, for the equilibrium volumes $\Omega_0 = \Omega(U = 0)$, which corresponds to $T = 0$ for alkali metals and to room temperature for alkaline-earth metals.

In calculating the shear constants $C_{ss'}$, we proceed from the 'force theorem' [26], as in [15]. According to this theorem, in the local density-functional (LDF) approximation the generalized force F_s corresponding to the deformation u_s may be written as

$$F_s = \frac{\partial E}{\partial u_s} = \sum_\lambda \Theta(\varepsilon_F - \varepsilon_\lambda)\left(\frac{\partial \varepsilon_\lambda}{\partial u_s}\right)_V + \int d^3r\, d^3r'\, \rho(r)\rho(r')\frac{\partial}{\partial u_s}\frac{1}{|r-r'|} = F_s^b + F_s^{es}. \tag{3}$$

Here ε_λ are one-electron energy levels in the crystal self-consistent potential $V(r)$; $\Theta(x)$ is a step function equal to 1 at $x > 0$ and to 0 at $x < 0$; while $(\partial\varepsilon_\lambda/\partial u_s)_V$ denotes a derivative of ε_λ at a 'frozen', i.e. unchanged, potential $V(r)$. According to the Hellman–Feynman theorem, the latter may also be expressed in terms of the derivative of the kinetic energy operator $\hat{T}$ (entering the LDF formalism):

$$(\partial\varepsilon_\lambda/\partial u_s)_V = \langle\lambda|\,\partial\hat{T}/\partial u_s\,|\lambda\rangle. \tag{4}$$

In the second term of equation (3), $\rho(r)$ is the total electric density of electrons and nuclei in the crystal ground state. Thus, according to equations (3) and (4), the F_s force has the visible form of the sum of two contributions of different nature: the 'band' term F_s^b relevant to the variation of the electron kinetic energy in the quantum Fermi occupation at the deformation u_s, and the second, 'electrostatic' term F_s^{es} connected with the change with u_s of the classical electrostatic energy at fixed density $\rho(r)$.

According to equation (1*a*), the shear constant $C_{ss'}$ is determined by the second derivative $\partial^2 E/\partial u_s\,\partial u_{s'}$. In this, no simple separation of contributions, analogous to equation (3), occurs and, in addition to the terms $C_{ss'}^b$ with derivatives at constant V and the 'electrostatic' ones $C_{ss'}^{es}$, there occur $C_{ss'}^m$ terms with mixed derivatives of the kinetic and potential energies:

$$C_{ss'} = C_{ss'}^b + C_{ss'}^m + C_{ss'}^{es} \tag{5a}$$

$$C_{ss'}^b = \frac{1}{N\Omega}\left[\sum_\lambda \Theta(-\xi_\lambda)\left(\frac{\partial^2\varepsilon_\lambda}{\partial u_s\,\partial u_{s'}}\right)_V - \sum_\lambda \delta(\xi_\lambda)\left(\frac{\partial\xi_\lambda}{\partial u_s}\right)_V\left(\frac{\partial\xi_\lambda}{\partial u_{s'}}\right)_V\right] \tag{5b}$$

$$C_{ss'}^m = \frac{1}{N\Omega}\left[\sum_\lambda \Theta(-\xi_\lambda)\int d^3r\, d^3r'\,\varphi_\lambda(r)\frac{\partial\hat{T}}{\partial u_s}\frac{\delta\varphi_\lambda(r)}{\delta V(r')}\frac{\partial V(r')}{\partial u_{s'}} - \sum_\lambda \delta(\xi_\lambda)\left(\frac{\partial\hat{T}}{\partial u_s}\right)_{\lambda\lambda}\left(\frac{\partial V}{\partial u_{s'}}\right)_{\lambda\lambda}\right] \tag{5c}$$

$$C_{ss'}^{es} = \partial F_s^{es}/\partial u_{s'} \tag{5d}$$

where $\xi_\lambda = \varepsilon_\lambda - \varepsilon_F$ and $\varphi_\lambda(r)$ is the one-electron wavefunction.

In using the LMTO-ASA method, the derivatives $(\partial\varepsilon_\lambda/\partial u_s)_V$ and $(\partial^2\varepsilon_\lambda/\partial u_s\,\partial u_{s'})_V$ entering into equation (5*b*) are determined by variation of only structural constants $S(k)$ with deformation u_s in the Hamiltonian (2*a*), while the potential parameters C_l, Δ_l and γ_l undergo no change and correspond to the self-consistent calculation in an undeformed crystal. This allows one to calculate these derivatives relatively easily by means of numerical differentiation of the ε_λ values obtained by diagonalization of the Hamiltonian H in equation (2) with $S(k)$ corresponding to the deformed lattice. At the same time, the presence of mixed derivatives in equation (5*c*) generally speaking requires self-consistent calculations in the deformed lattice [27], which are much more difficult. However, a calculation of this type performed by Christensen [15] for Pd and Au showed

that in the C' constant considered by him the contributions of the $C^{m}_{ss'}$ terms were negligible compared with those of the $C^{b}_{ss'}$ term. This may reflect the smallness of contributions made by the non-spherically symmetrical components of the muffin-tin potential, $\partial V/\partial u_s$, to the $\partial \varepsilon_\lambda/\partial u_s$ values, compared with those made by $\partial \hat{T}/\partial u_s \sim \partial S(k)/\partial u_s$. Since, in addition, in this work we are mainly interested in only qualitative effects, the $C^{m}_{ss'}$ contributions will be omitted below.

The quantitative calculation of the $C^{es}_{ss'}$ term (5*d*) also requires considerable efforts [15]. But proceeding from the physical considerations mentioned in section 1 one may assume that the band anomalies in $C_{ss'}(U)$, in which we are interested, are determined mainly by the 'band' contribution $C^{b}_{ss'}$, while $C^{es}_{ss'}$ can be interpolated by a smooth function of the volume Ω. In the same way as in [19] we assume this function to be proportional to the Madelung contribution $C^{Mad}_{ss'}$ to the shear constant:

$$C^{es}_{ss'} = AC^{Mad}_{ss'}(Z, \Omega) \qquad C^{Mad}_{ss'} = b_{ss'} Z^2 e^2 \Omega^{-4/3}. \tag{6}$$

Here A is an empirical constant; Z is the valence; while $b_{ss'}$ are numerical coefficients determined by the lattice geometry only. For the $C' = \frac{1}{2}(C_{11} - C_{12})$ and C_{44} constants in the BCC and FCC structures considered below, these coefficients are given in table 1.

In calculating the band term $C^{b}_{ss'}$ we used the procedure described in [3]. The C' constant corresponds to the tetragonal deformation η_1, while C_{44} corresponds to the trigonal one η_2. Their corresponding deformation matrices a_1 and a_2 have the form

$$a_1 = \begin{pmatrix} \xi_1^{-1/3} & 0 & 0 \\ 0 & \xi_1^{-1/3} & 0 \\ 0 & 0 & \xi_1^{2/3} \end{pmatrix} \qquad a_2 = \tfrac{1}{3}\xi_2^{-1/3}\begin{pmatrix} \xi_2 + 2 & \xi_2 - 1 & \xi_2 - 1 \\ \xi_2 - 1 & \xi_2 + 2 & \xi_2 - 1 \\ \xi_2 - 1 & \xi_2 - 1 & \xi_2 + 2 \end{pmatrix} \tag{7}$$

where $\xi_i = (1 + \eta_i)^{-1}$. If, for brevity, we use C_1 to denote the C' constant and C_2 for C_{44}, the explicit expressions for the $C^{b}_{ss'}$ in (5*b*) take the form

$$C^{b}_{i}(\varepsilon_F) = C^{bv}_{i}(\varepsilon_F) + C^{bs}_{i}(\varepsilon_F)$$

$$= \tfrac{3}{4}\sum_n \int \frac{d^3k}{4\pi^3}\left[\Theta(\varepsilon_F - \varepsilon_{nk})\frac{\partial^2 \varepsilon_{nk}}{\partial \eta_i^2} - \delta(\varepsilon_{nk} - \varepsilon_F)\left(\frac{\partial \varepsilon_{nk}}{\partial \eta_i}\right)^2\right]. \tag{8}$$

Here ε_{nk} is the energy of the state with quasi-momentum k in the nth band, while C^{bv}_{i} and C^{bs}_{i} correspond to the first and second terms in the square brackets in equation (8), i.e. to the contributions of the states in the Fermi occupation volume and on the Fermi surface, respectively. If we substitute the variable ε for ε_F in equation (8), the function $C^{bs}_{i}(\varepsilon)$ scales with the density of states $n(\varepsilon)$ (differing from it only in the $-\frac{3}{4}(\partial \varepsilon_{nk}/\partial \eta_i)^2$ factor under the integral sign), while C^{bv}_{i} scales with the number of states $N(\varepsilon)$, defined as

$$N(\varepsilon) = \int^{\varepsilon} d\varepsilon'\, n(\varepsilon'). \tag{9}$$

Table 1. Values of $b_{ss'}$ coefficients in relation (6).

Structure	BCC	FCC
$b' = \frac{1}{2}(b_{11} - b_{12})$	0.039 58	0.033 33
b_{44}	0.294 62	0.298 70

Therefore, the character of singularities in ε (e.g. the Van Hove ones) for the C_i^{bs} and $n(\varepsilon)$ functions, as well as for the C_i^{bv} and $N(\varepsilon)$ functions, is the same; see figures 2–4 and 10–13 below.

To calculate C', we used the body-centred tetragonal (BCT) lattice, in which the tetragonality parameter value $c/a = 1$ corresponds to the BCC structure, while $c/a = \sqrt{2}$ corresponds to the FCC one. The C_{44} constant was calculated within the trigonal lattice, for which $c/a = \frac{1}{3}\sqrt{6}$ corresponds to the BCC and $c/a = \sqrt{6}$ to the FCC structures. The derivatives with respect to η_i in equation (8) were found by numerical differentiation of the band energies ε_{nk} over five points corresponding to steps of $\Delta(c/a) = 0, 0.01$ and 0.02. In numerical integration by the tetrahedron method, the number of k-points in the irreducible part of the Brillouin zone (BZ) was taken to be 104 for the BCC and FCC structures, 244 for the BCT structure and 288 for the trigonal structure, which in all cases corresponded to 3375 points in the total BZ (having the same volume $8\pi^3/\Omega$ in all the structures).

Let us discuss the A value in the interpolation (6). It will be seen from what follows that for all the metals considered in this paper the choice of the same $A = 5/3$ value usually results in good agreement with the available experiments. Therefore, we shall use only $A = 5/3$ below. We now give some considerations in favour of the possibility that with $A = 5/3$ relations of the type of equation (6) are approximately fulfilled. As mentioned in section 1, the E_{es} value in equation (1*b*) is the difference $E_{Mad} - U_{ee}$. If the $C^b_{ss'}$ term had corresponded to the total $\partial^2 E_b/\partial u_s\,\partial u_{s'}$ derivative of the band energy E_b in equation (1*b*) (rather than to the derivative at constant potential, as in our actual calculations by equation (5*b*)) and if, in finding $C^{es}_{ss'} = \partial^2 E_{es}/\partial u_s\,\partial u_{s'}$ in equation (1*b*), only the purely electrostatic contribution U^{es}_{ee} was taken into account in U_{ee} (disregarding the exchange–correlation one U^{xc}_{ee}), the value $A = 5/3$ in equation (6) would have corresponded to the relation

$$(\partial^2/\partial u_s\,\partial u_{s'})\,E_{es} = (\partial^2/\partial u_s\,\partial u_{s'})\,(E_{Mad} - U^{es}_{ee}) = \tfrac{5}{3}(\partial^2/\partial u_s\,\partial u_{s'})\,E_{Mad}. \tag{10}$$

Now, if we make use of the known estimate of the electrostatic energies in the neutral spherical Wigner–Seitz cell with constant electron density Z/Ω and point charge Z at its centre for U^{es}_{ee} and E_{Mad} in equation (10) (see e.g. [28]) then we obtain $E_{Mad} - U^{es}_{ee} = \frac{5}{3}E_{Mad}$. Therefore, in the absence of differentiation in equation (10), the approximate fulfilment of this equality could be considered natural. We cannot prove an analogous relation immediately for the derivatives entering into equation (10), nor can we substantiate the insignificance of the terms with $\partial V/\partial u_s$ and with U^{xc}_{ee}. However, the presented considerations allow us to assume that the approximate fulfilment of the relations of the type of equation (6) with $A = 5/3$ is possible, at least for some classes of metals.

3. Changes of electronic structure under compression and their influence on structural stability

Variations of the electronic structure of the considered metals under compression are illustrated in figures 1–4. Let us discuss these variations.

The $n(\varepsilon, U)$ dependences in the BCC Li and Na (figure 1) were considered earlier [7] and are given here for completeness of the discussion. These metals display a simple band

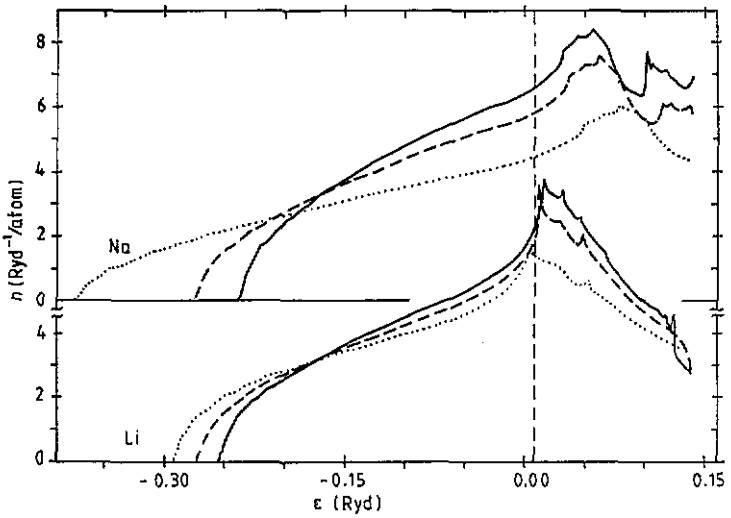

Figure 1. The electron density of states $n(\varepsilon)$ for BCC Li and BCC Na. The vertical broken line here and in other figures indicates the Fermi level ε_F. The full, broken and dotted curves correspond to the compressions $U = 0$, 0.2 and 0.5.

structure formed by the s and p states, with the $n(\varepsilon)$ peak at the ε_c point corresponding to the Van Hove singularity at the point N of the BZ. The $\Delta_{cF} = \varepsilon_c - \varepsilon_F$ distance in Na increases with U, in compliance with the nearly free electron (NFE) character of the band structure: $\Delta_{cF} \sim \Omega^{-2/3}$. Thus the $n(\varepsilon)$ singularity at $\varepsilon = \varepsilon_c$ does not manifest itself in the ground-state properties of Na. On the contrary, in Li the presence of strong, resonance-like attraction for the p states corresponding to the point N results in a relatively weak dependence of the ε_c value on compression, while the energies of the NFE s states (which, mainly, determine the ε_F value) increase with U as $(\Omega_0/\Omega)^{2/3} = (1 - U)^{-2/3}$. As a result, in BCC Li the Δ_{cF} value drops with rising U and the Fermi level creeps over the peak in $n(\varepsilon)$. This causes increase in the band energy and loss of stability of the BCC phase as compared with the closed-packed ones (HCP, FCC, 9R, etc. [7]). This 'band' tendency to structural instability is also manifested in the considerable softening of the shear constants; see [7, 17, 18] and figure 5 below.

The variation of the band structure of Cs under pressure was discussed by many authors; see e.g. [21]. Our results presented in figure 2 basically agree with the previous ones. They describe the main feature of this variation, which is also characteristic of alkaline-earth metals: the decrease of the resonance d band energy relative to that of the s and p states (which is analogous to the situation mentioned in Li). In caesium, with increasing U, this causes the Fermi level ε_F to get into the d band and relevant structural phase transitions appear. Thus, according to figure 2, at $U > 0.3$, ε_F in FCC Cs falls within the pseudogap (corresponding to the vicinity of point X in the BZ). As discussed by Skriver [21], on further increase of U this induces the conventional 'band' mechanism for the transition from BCC to FCC phase, which is observed experimentally at $U = U_c^{exp} \simeq 0.4$ [29].

The results for $n(\varepsilon, U)$ in Sr and Ba are shown in figures 3 and 4; for Ca they are generally similar to those for Sr. For the earlier investigated cases of FCC Ca and Sr at $U = 0$ [12] and BCC Ba at $U = 0$ and $U = 0.3$ [22], our $n(\varepsilon)$ are close to those obtained

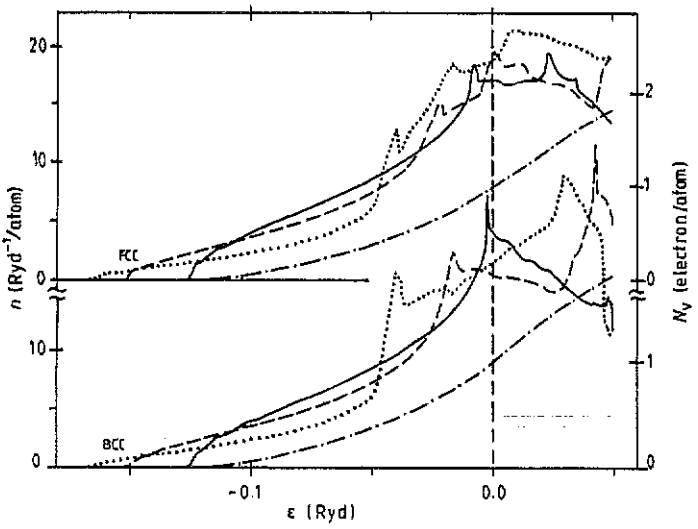

Figure 2. Plots of $n(\varepsilon)$ and the number of states $N(\varepsilon)$ (see equation (9)) for BCC and FCC Cs. The full, broken and dotted curves correspond to $n(\varepsilon)$ at $U = 0$, 0.3 and 0.5; the chain curve is $N(\varepsilon)$ at $U = 0$.

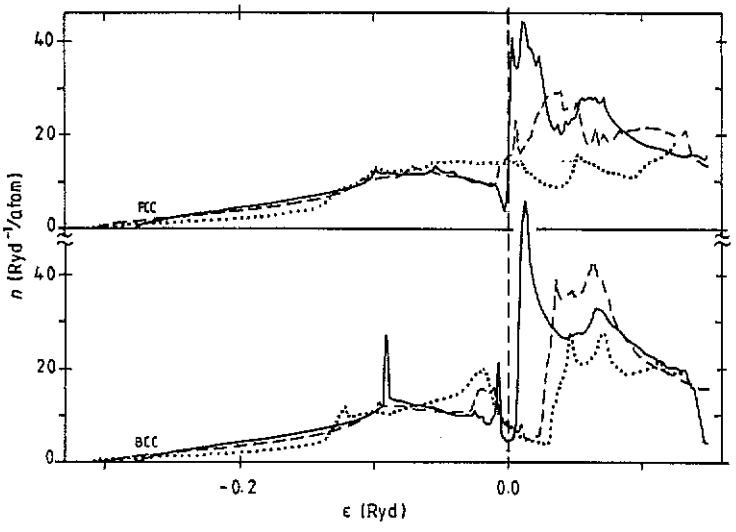

Figure 3. Plots of $n(\varepsilon)$ for BCC and FCC Sr. The full, broken and dotted curves correspond to $U = 0$, 0.25 and 0.5.

earlier. With rising U, the above-mentioned decrease of the energy of d states (relative to the s and p states) results in significant changes of the band structure, in the course of which ε_F passes a number of singular points, peaks and dips in $n(\varepsilon)$. These variations, illustrated by figures 3 and 4, correlate with the presence of a number of structural phase transitions in the alkaline-earth metals under pressure [20].

For Ba these correlations can be followed most clearly. At $U = 0$, ε_F in Ba lies

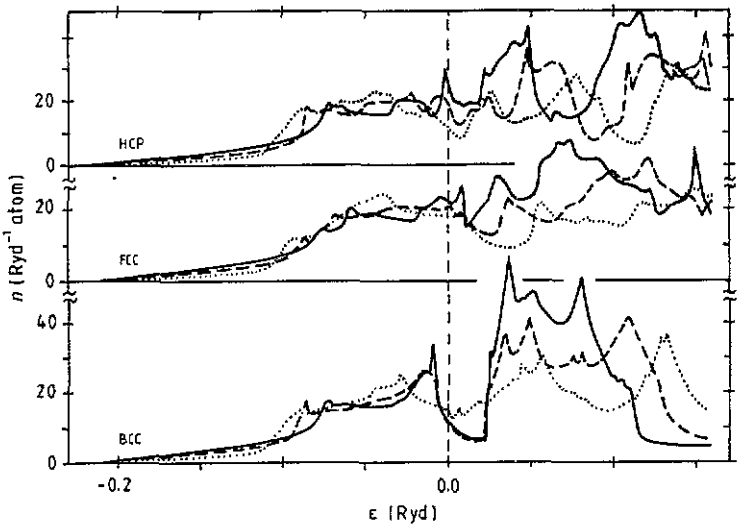

Figure 4. Plots of $n(\varepsilon)$ for BCC, FCC and HCP Ba. The full, broken and dotted curves correspond to $U = 0$, 0.2 and 0.35.

between the two peaks of $n(\varepsilon)$ (having mainly d symmetry) and with rising U these peaks start to get shifted to the left. At small $U \leqslant 0.3$, ε_F in the BCC phase still lies in the vicinity of the $n(\varepsilon)$ minimum, while in the FCC and HCP ones it lies near its maximum, which evidently determines the observed stability of the BCC phase at small U. However, at $U > 0.3$, ε_F in the BCC phase (as in the FCC one) turns out to be in the vicinity of the maximum, while in the HCP one it is close to the $n(\varepsilon)$ minimum. In addition, the broad peak of occupied states in the HCP phase has somewhat lower energy than that in the BCC phase. Apparently, it is the resulting 'band' gain in the energy that induces the structural BCC–HCP transition (which is observed in Ba at $U_c^{exp} \simeq 0.32$ [5]).

In Sr (and Ca) at $U = 0$, ε_F lies lower than the main $n(\varepsilon)$ peak corresponding to the hybridized d and p states. With rising U the d states of this peak are mainly shifted to the left, while the p states are shifted to the right, which results in the complicated change of $n(\varepsilon)$ with U near ε_F in figure 3. So, for small $U < 0.2$, the form of $n(\varepsilon)$ at $\varepsilon < \varepsilon_F$ is similar in the FCC and BCC phases, so that the study of their energetic preference requires quantitative calculations (see e.g. [21]). However, at $U \geqslant 0.2$, in FCC Sr $n(\varepsilon_F)$ starts to increase sharply due to ε_F creeping over the $n(\varepsilon)$ peak, while for the BCC phase ε_F remains at the $n(\varepsilon)$ minimum. This correlates with the presence of the FCC–BCC transition in Sr at $U_c^{exp} \simeq 0.2$ [6]. For Ca the creeping of ε_F over the $n(\varepsilon)$ peak takes place at larger U, which correlates with the larger value of $U_c^{exp} \simeq 0.38$ for the FCC–BCC transition in Ca [20].

In the next section we shall show that the discussed $n(\varepsilon)$ variations also cause sharp anomalies in the shear constants $C_{ss'}(U)$, in particular in the vicinity of the points of the structural phase transitions.

4. Variation of shear constants under pressure

In figures 5–9 we present the calculated $C_{ss'}(U)$ dependences for the BCC or FCC

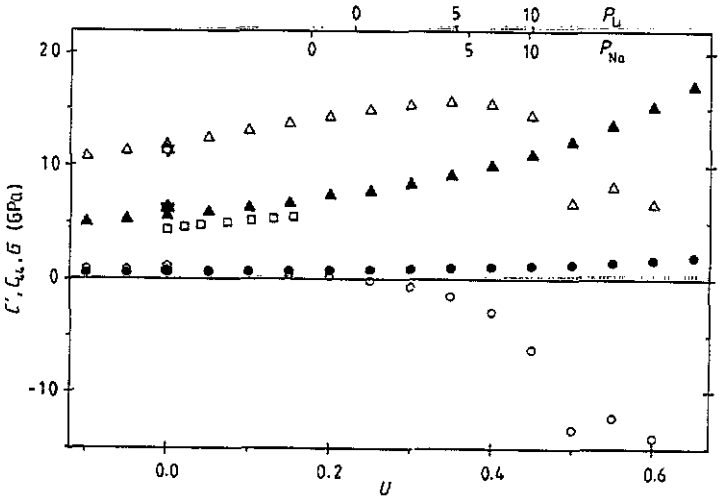

Figure 5. The shear constants in the BCC phase of Li and Na versus U. The open symbols correspond to Li, the full ones to Na. Calculations: triangles, C_{44}; circles, C'. Experiments: stars, C_{44} at $U = 0$; pentagons, C' at $U = 0$; squares, experimental $G(U)$ for polycrystalline Li samples [6]. The calculated pressure values p are given in GPa.

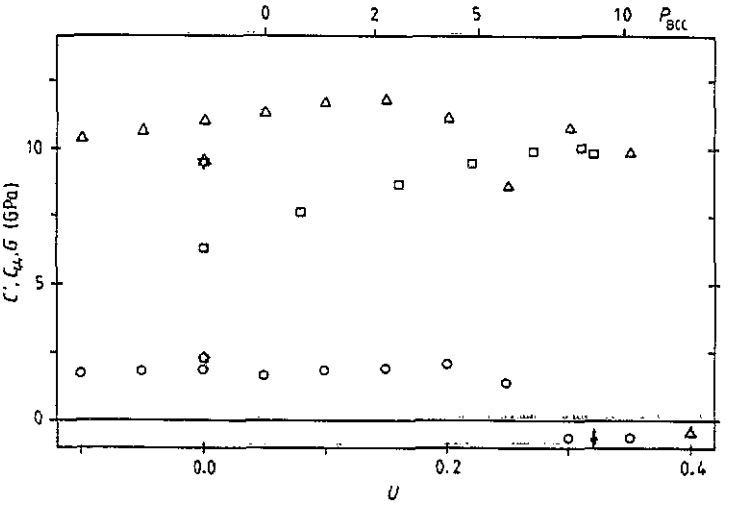

Figure 6. The shear constants in BCC Ba versus U. The notation is the same as in figure 5 for Li. Experimental $G(U)$ are taken from [4]. The arrows in figures 6–9 indicate the experimental phase transition points $U = U_c$.

phases of Li, Na, Cs, Ca, Sr and Ba, together with the available experimental data. In these figures the experimental $C_{ss}(U = 0)$ for alkali metals correspond to $T = 0$ and are taken from table 1 in [30], while for the alkaline-earth metals they correspond to $T = 295$ K and are taken from table 2 in [31]. The arrows on the abscissa indicate values $U = U_c^{exp}$ of the structural phase transition points (for the lower-pressure phase). For Li, at $T = 0$ the 9R phase is the equilibrium phase instead of the BCC one, while at room temperature the transition from the BCC to that (or another) phase occurs at $U_c^{exp} \approx$

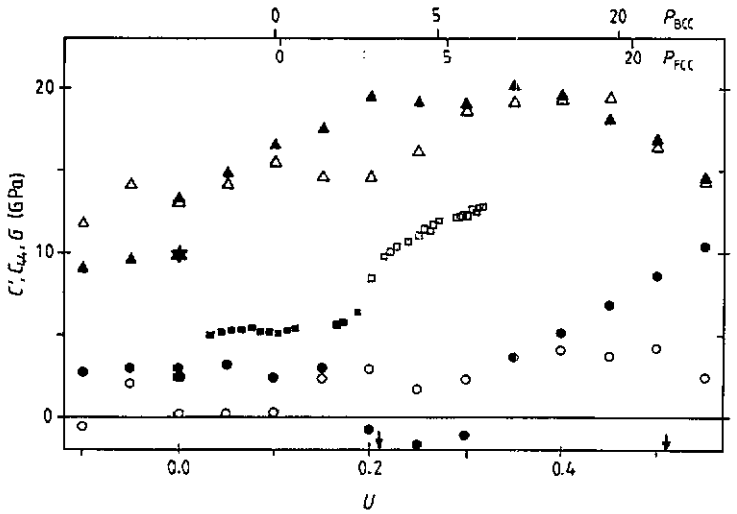

Figure 7. The shear constants in Sr versus U. The open symbols correspond to the BCC phase; the full ones to the FCC phase. Experimental $G(U)$ are taken from [5].

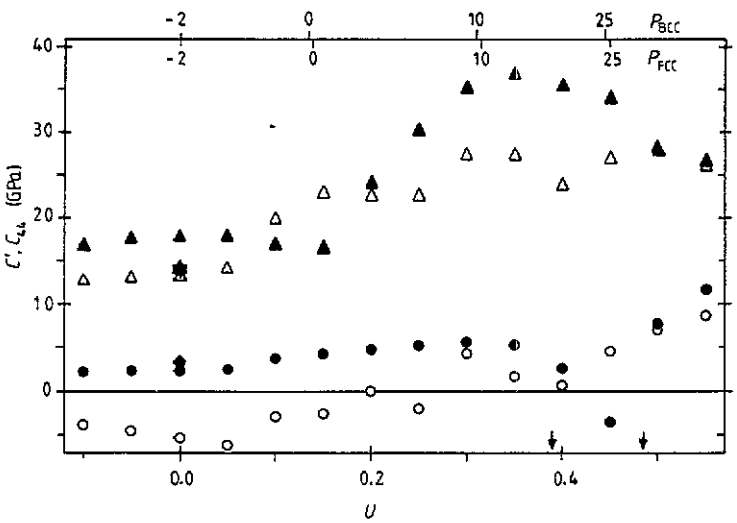

Figure 8. The same as figure 7 but for Ca.

0.3 [7]. Note also that the results for $n(\varepsilon)$ and $C'(U)$ in Na and Li, given in figures 1 and 5, differ somewhat from those in figures 6 and 7 of [7] due to some changes in details of calculations in the present work (the choice of another approximation for $V^{xc}(r)$, the increased number of k-points in integration over the BZ, etc).

Figures 10–13 illustrate the form of various contributions, $C_{ss'}^{bv}$, $C_{ss'}^{bs}$ and $C_{ss'}^{b} = C_{ss'}^{bv} + C_{ss'}^{bs}$ to the total $C_{ss'}$. Instead of the $C_{ss'}^{b}(\varepsilon_F)$ values determined by equation (8), we (in the same way as Ohta and Shimizu [3]) present the $C_{ss'}^{b}(N_v)$ functions of the number of occupied states in the valence band, $N_v = N(\varepsilon_F)$, with $N(\varepsilon)$ given by equation

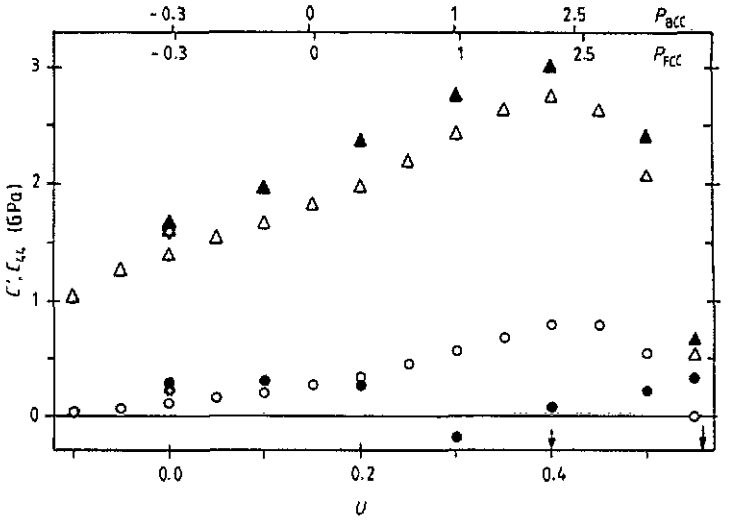

Figure 9. The same as figure 7 but for Cs.

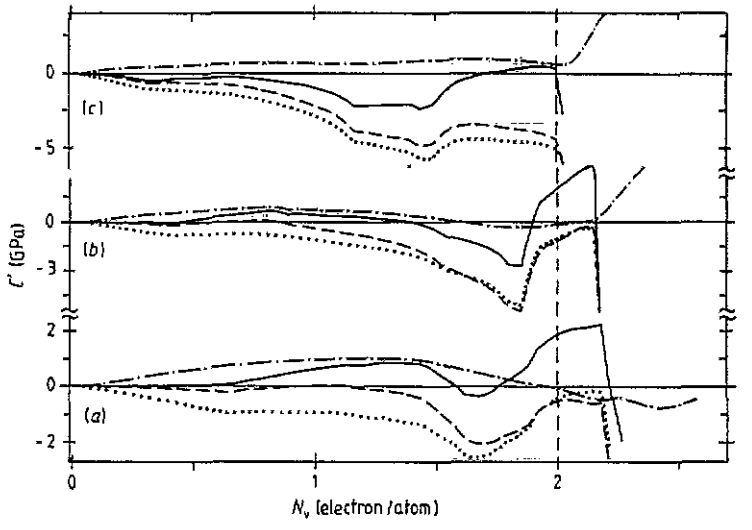

Figure 10. The different contributions to the shear constant $C'(U)$ in BCC Ba: (*a*) $U = 0$; (*b*) $U = 0.2$; (*c*) $U = 0.35$. Here and in figures 11–13 the dotted, chain, broken and full curves correspond to the terms $C^{bs}_{ss'}$, $C^{bs}_{ss'}$, $C^{b}_{ss'}$ and $C^{total}_{ss'} = C^{b}_{ss'} + C^{es}_{ss'}$, respectively. The term $C^{es}_{ss'}$ is calculated according to equation (6), substituting N_v for Z.

(10). For the pure metals discussed in this paper N_v is their valence Z, i.e. 1 or 2. However, the consideration of arbitrary $N_v \neq Z$ allows us to follow the evolution of the band singularities in $C^{b}_{ss'}$ with N_v and to obtain qualitative information (in the rigid-band approximation) on the character of the $C_{ss'}$ variation in alloys, e.g. Ba–Cs or Ba–La. The correspondence of the ε values in figures 2–4 with N_v in figures 10–13 is illustrated by the curve $N(\varepsilon) = N_v(\varepsilon)$ in figure 2.

Finally, figures 14 and 15 illustrate the dependence of total $C_{ss'} = C^{b}_{ss'} + C^{es}_{ss'}$ on two

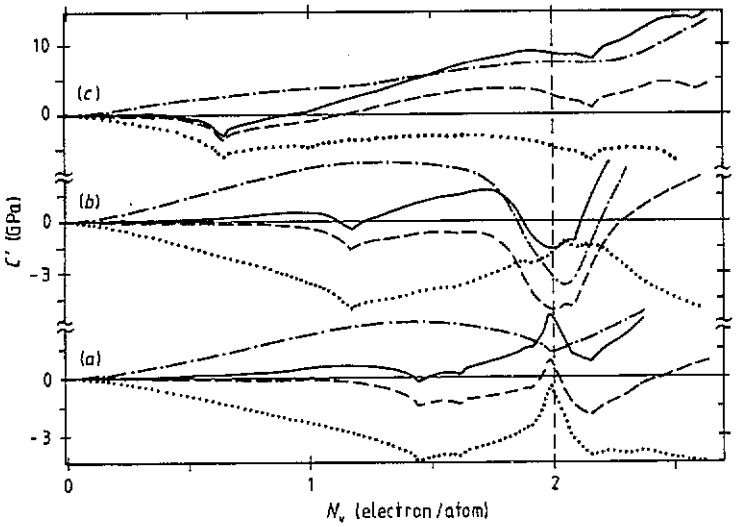

Figure 11. The same as figure 10 but for C' in FCC Sr: (*a*) $U = 0$; (*b*) $U = 0.25$; (*c*) $U = 0.5$.

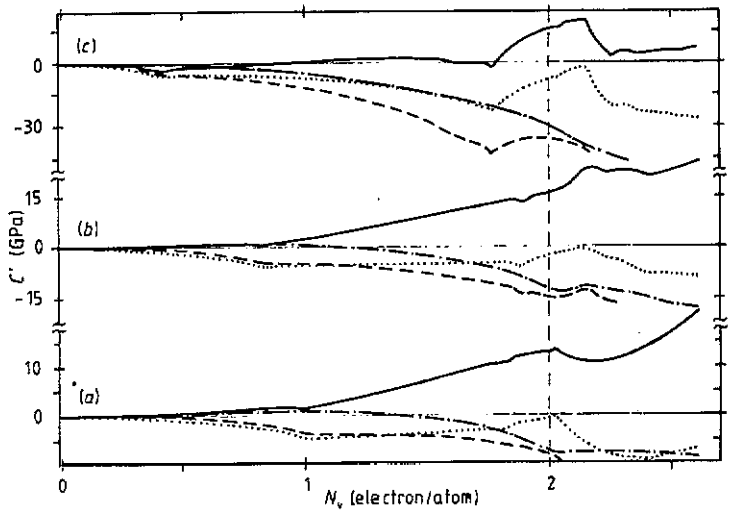

Figure 12. The same as figure 11 but for C_{44} in BCC Sr.

parameters, the compression U and number of electrons N_v. Here $C_{ss'}^{es}$ is calculated according to equation (6) substituting N_v for Z, in compliance with the mentioned possibility of applying the results to alloys. The lower part of these figures also illustrates the connection of the anomalies in $C_{ss'}$ with the proximity of ε_F to the van Hove singularity points.

Let us discuss the results presented. Note first, that at $U = 0$ the calculated $C_{ss'}$ values in figures 5–8 are usually in good agreement with the observed ones. But for BCC Cs using $Z = 1$ in equation (6) yields $C_{44} = 0.8$ and $C' = 0.03$ GPa instead of the experimental values of 1.6 and 0.22, respectively. However, if in calculating the elec-

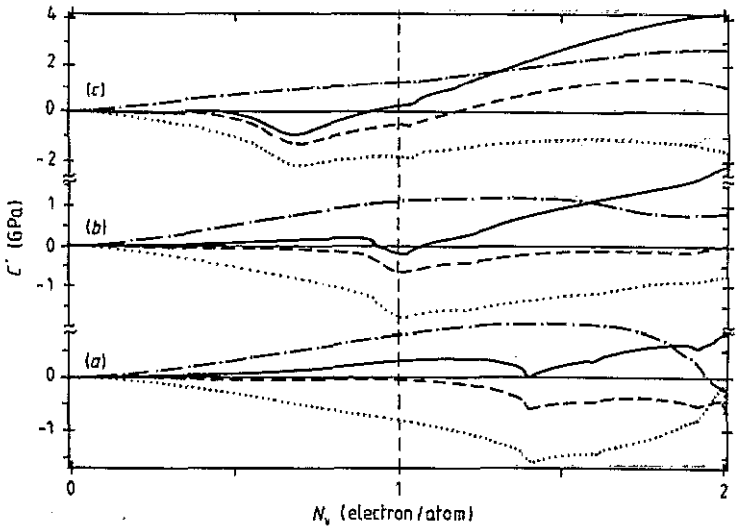

Figure 13. The same as figure 10 but for C' in FCC Cs: (*a*) $U = 0$; (*b*) $U = 0.3$; (*c*) $U = 0.5$. The C'_{es} term is calculated substituting $Z_0 N_v = 1.123 N_v$ for Z in equation (6); see the text.

trostatic contribution (6) one allows for the noticeable overlap of the ion cores in Cs and, instead of the nominal valence $Z = 1$, one uses, e.g. the value of $Z_0 = 1.123$ proposed for Cs by Dacorogna *et al* [19] (they estimated this value from the relation for the electron density in the interstitial space, $\psi^2(S) = Z_0/\Omega$, where $\psi(S)$ is the electron wavefunction value within the LMTO-ASA approximation at the Wigner–Seitz boundary), one has $C_{44} = 1.4$ and $C' = 0.11$ GPa. Taking into account the strong compensation for the $(C')^{es} = C'_{es}$ and $(C')^{b} = C'_{b}$ contributions in Cs ($C'_{b} = -0.26$ GPa), the agreement with experiment can now be considered to be satisfactory. Thus, to describe $C_{ss'}$ in Cs more realistically, the $C^{es}_{ss'}$ values for Cs presented in figures 6 and 13 were calculated at $Z = Z_0 = 1.123$ in equation (6).

At $U = 0$ the comparison of the calculations with the data on averaged shear constants $G(U)$ in polycrystalline Ba, Sr and Li [4–6] is hindered by the known uncertainty in the connection of this G with the C' and C_{44} values for anisotropic crystals. However, note that the calculated values of compressions $U = U_s$ corresponding to the sharp decrease or vanishing of one or both shear constants $C_{ss'}$ in figures 5–9 turn out, as a rule, to be close to the observed phase transition point values $U_c^{exp} = U_c$. Only for Li is the calculated (with recalculation to the room-temperature value $\Omega = \Omega(T = T_r = 295\,\mathrm{K})$) $U_s \simeq 0.25$ somewhat underestimated as compared with the $U_c(T_r) \simeq 0.3$. Apparently, this reflects the general underestimation of our calculated C' for Li. However, for the $C_{ss'}$ values in Li the temperature and zero-point motion effects disregarded by us can be important [7, 32].

Figures 10–13 illustrate the relative importance and character of the $C^{bv}_{ss'}$ and $C^{bs}_{ss'}$ contributions to the total band $C^{b}_{ss'}$. One can see, in particular, that the 'Fermi surface' $C^{b}_{ss'}$ terms are often the main ones and that they change with N_v or with ε in much the same way (and oppositely in sign) as the density of states $n(\varepsilon)$ in figures 2–4, in compliance with the mentioned analogy between these quantities. However, the $C^{b}_{ss'}$ function variations (e.g. near the points of the $n(\varepsilon)$ singularities) are usually much sharper than

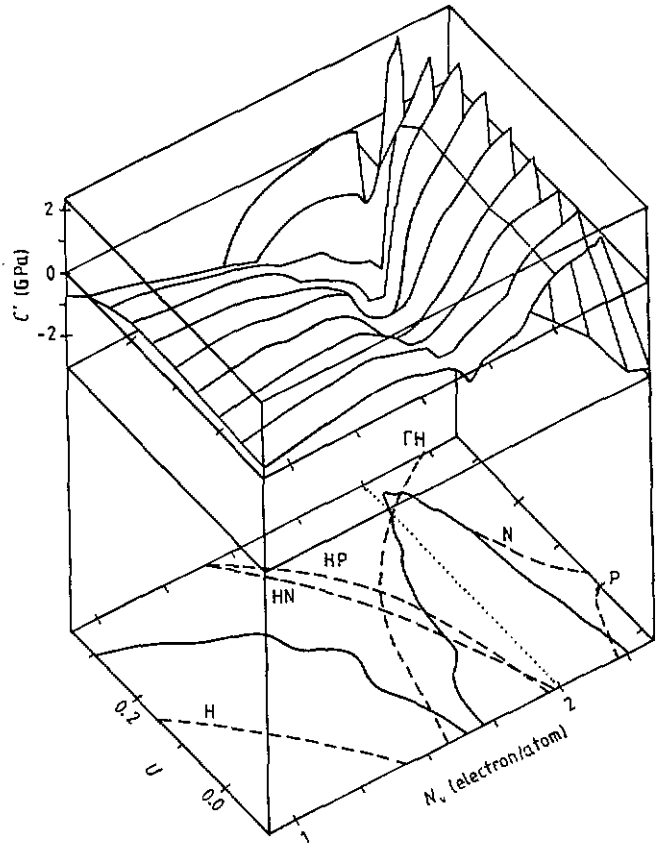

Figure 14. The upper part presents the function $C'(N_v, U)$ and the lower part the (N_v, U) plane for BCC Ba. In the (N_v, U) plane the full curves correspond to the equation $C'(N_v, U) = 0$; the broken curves with index i denote the trajectories of the Van Hove singularities corresponding to point i in the BZ, and those with index i, j to 'accidental' (being not symmetry-induced) Van Hove points belonging to line ij in the BZ.

those in $n(\varepsilon)$. This reflects the importance of the geometrical effects of the Fermi surface form variation in anisotropic characteristics such as the shear constants [17, 18].

Let us discuss the $C_{ss'}(U)$ dependences for separate metals. For Na these dependences presented in figure 5 are close to those calculated within the pseudopotential perturbation theory [7] and for $U \leqslant 0.1$ they are also close to the experimental $C_{ss'}(U)$ [32]. Here the $C_{ss'}$ grow smoothly and monotonically with U, which reflects the absence of singularities in $n(\varepsilon)$ at $\varepsilon \leqslant \varepsilon_F$. On the contrary, in BCC Li, ε_F with rising U approaches the ε_c point of the $n(\varepsilon)$ peak, and the structural stability decrease connected with that manifests itself in a sharp drop of the C' constant (which related to the BCC–close packed phase transitions). It is seen from table 2 that this decrease of C' in Li is entirely determined by the Fermi surface band contribution C'_{bs}, which changes most sharply with decreasing $\varepsilon_F - \varepsilon_c$. In the C_{44} constant in Li this softening (at small $U \leqslant 0.25$) manifests itself much more weakly, though being displayed in the form of negative curvature of the $C_{44}(U)$ function (unlike Na where this curvature is positive). The discussed band effects also account for the known considerable overestimation of the

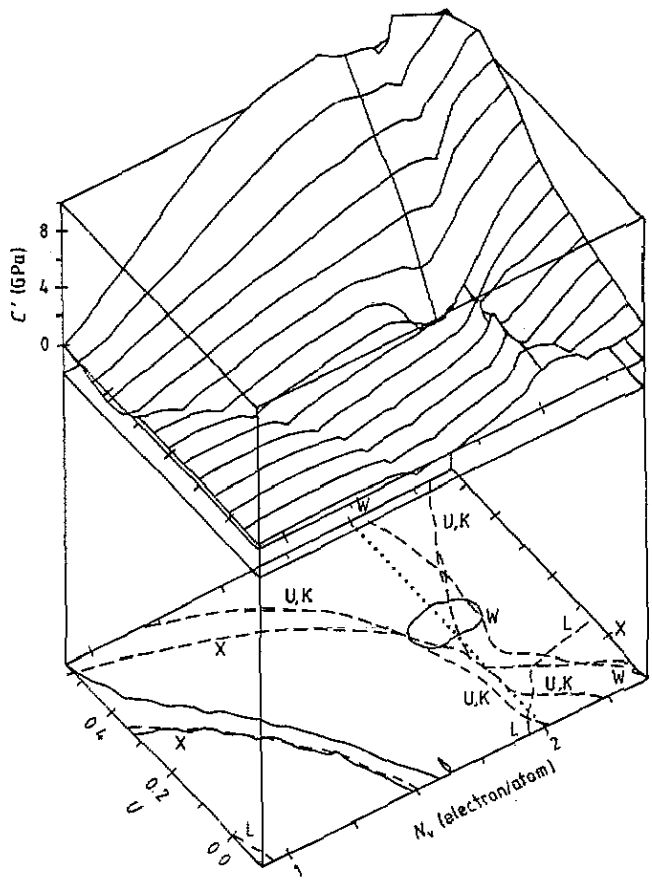

Figure 15. The same as figure 14 but for C' in FCC Sr.

values of the $\partial C_{ss'}/\partial p$ derivatives for Li in the pseudopotential perturbation theory calculations [30].

Variation of the $C_{ss'}$ with U for Ba (figures 6, 10 and 14) is more complicated than for Li, in compliance with the more complicated change of the band structure. Table 2 shows that here also the main change of C' is usually determined by the surface term C'_{bs}. However, in transition from $U = 0.2$ to $U = 0.25$, the great $\delta C'_{bv}$ change is realized at a relatively small $\delta C'_{bs}$. One can see from figure 4 that the $n(\varepsilon)$ variation in this case is mainly connected with changing shape of the occupied d peak, i.e. it occurs mainly in the volume rather than on the surface of Fermi occupation; this results in precisely the $|\delta C'_{bv}| \gg |\delta C'_{bs}|$ values. This example, as well as others to be discussed below, shows that if the change in the electronic structure with external parameters (pressure, concentration in an alloy, etc) corresponds with a considerable change of $n(\varepsilon)$ at $\varepsilon < \varepsilon_F$ (unlike the rigid-band model), this can also sharply vary the atomic (in particular, the elastic) properties. This can explain, for example, the unusual concentration anomalies of the strength properties of the Fe_xCr_{1-x} alloys in which the band structure varies with x in an appreciably 'not rigid' way [33].

The results for Ba in table 2 also illustrate the mentioned enhancement of singularities

in the band contribution $C_{ss'}^{bs}$ as compared with those in $n(\varepsilon_F)$. Thus, in transition from $U = 0.2$ to $U = 0.3$, the $n(\varepsilon_F)$ value in figure 4 increases by only 20–25%, while the $(-C'_{bs})$ term increases by almost a factor of 5. Figures 10 and 14 also show that the loss of stability for BCC Ba at $U \geqslant 0.3$ is connected with ε_F approaching the point ε_c corresponding to the states near the point N in the BZ, as in the BCC Li case. However, in Ba the d-type states (rather than the p-type ones, as in Li) are 'critical', for which a number of flat ε_{nk} branches in the BZ, such as, e.g. the N–P branch [22], are characteristic. The result is a sharper singularity of the $n(\varepsilon_F)$ and $C_{ss'}^{bs}$ functions than in Li, and correspondingly a sharper decrease of the $C'(U)$ in figure 6 when U approaches U_c.

The results for $C_{ss'}(U, N_v)$ in Sr and Ca are qualitatively similar and mainly differ in quantitative details. Figures 7 and 8 show, first, that our $C_{ss'}$ calculations for the BCC and FCC phases correlate well with the data on the structural stability of Sr and Ca. It is seen that, at $U < U_{c1}$, the experimental value for the transition from the FCC phase to the BCC one, the calculated C' values in the BCC phase are rather small or negative, while at $U \geqslant U_{c1}$, on the contrary, the C' values for the FCC phase become negative. One can also see that on further increase of U in BCC Sr and as it approaches the U_{c2} point of the second structural transition (from BCC to a certain undetermined phase), there occurs a sharp drop of the C_{44} constant, while in $C'(U)$ the softening is less pronounced. This may reflect a tendency for going over into some more complicated structure, e.g. that of the Cs-IV type in caesium (for which we obtained an analogous drop of the calculated $C_{44}(U)$ at $U > 0.4$; see figure 9).

Figures 7, 11, 12 and 15 and table 2 show that in Sr the discussed band effects in

Table 2. Contributions to $C'(U)$ constant (GPa).

Metal, structure	$U = (\Omega_0 - \Omega)/\Omega_0$	C'_{bv}	C'_{bs}	C'_b	C'_{es}	C'
Na, BCC	0	5.1	−5.7	−0.6	1.2	0.6
	0.2	7.2	−8.1	−0.8	1.6	0.8
Li, BCC	0	9.7	−11.5	−1.8	2.6	0.8
	0.2	13.4	−16.7	−3.3	3.5	0.2
	0.3	16.3	−21.1	−4.8	4.2	−0.7
Ba, BCC	0	−0.1	−0.4	−0.5	2.4	1.9
	0.1	−0.3	−0.6	−0.9	2.8	1.9
	0.2	−0.1	−1.0	−1.1	3.3	2.1
	0.25	−0.9	−1.2	−2.1	3.5	1.4
	0.3	0.1	−4.6	−4.5	3.9	−0.6
Sr, FCC	0	1.4	−0.8	0.5	2.4	2.9
	0.05	1.4	−0.9	0.5	2.5	3.1
	0.1	0.9	−1.2	−0.3	2.7	2.5
	0.15	0.6	−0.6	0.0	3.0	3.0
	0.2	−3.0	−0.9	−3.9	3.2	−0.7
	0.3	0.4	−3.1	−2.8	3.8	1.1
Sr, BCC	0	−2.2	−0.4	−2.6	2.8	0.2
	0.1	−2.1	−0.7	−2.8	3.3	0.4
	0.15	−0.2	−1.0	−1.1	3.5	2.4
	0.3	−1.2	−1.0	−2.2	4.5	2.3

$C_{ss'}(U)$ manifest themselves very clearly. This is connected with the fact that a number of the ε_c points of the Van Hove singularities in $n(\varepsilon)$ are located in the vicinity of ε_F, and the $\varepsilon_F - \varepsilon_c$ values vary considerably with changing U. The variations in $C^b_{ss'}$ again are much greater than those in $n(\varepsilon_F)$. Thus, in changing U from 0.05 to 0.1 in FCC Sr, when the energies ε_c(K) and ε_c(X) of the states corresponding to the points K and X in the BZ get through ε_F (figure 15), $n(\varepsilon_F)$ changes only by 5%, while the C'_b value in table 2 drops from 0.5 down to −0.3 GPa. Note that in the $G(U)$ dependence for polycrystalline Sr, a certain minimum is also noticeable in figure 7 near $U = 0.1$, which may correspond to the discussed 'band' minimum in $C'(U)$. At $U \simeq 0.2$ the $\varepsilon_c(K)$ energy in FCC Sr again passes through ε_F (figure 15). Together with the other changes in the band structure (figure 3) this results in a sharp drop of C' down to negative values, i.e. in a loss of FCC phase stability.

The results for Sr also illustrate the mentioned possibility of the sharp variation of the 'bulk' $C^{bv}_{ss'}$ term. This takes place in the FCC phase of Sr for C' close to $U = 0.2$, and in the BCC phase for C' close to $U = 0.15$ and for C_{44} close to $U = 0.4$–0.5. Note also that the decrease of $C_{44}(U)$ at large $U \geqslant 0.5$ in Sr, Ca and Cs (figures 7–9 and 12) is mainly due to the drop of just the bulk C^{bv}_{44} contribution. For comparison, recall that in the calculations [3] for BCC d metals the sharpest anomaly in the $C^b_{44}(N_v)$ dependence (corresponding to the V–Cr alloys) was also determined by the bulk C^{bv}_{44} contribution, so that such anomalies may be a sufficiently general band effect.

The $C_{ss'}(U)$ dependences for Cs presented in figures 9 and 13 differ somewhat from other metals. When U in the BCC phase approaches point $U_{c1} \simeq 0.4$ of the observed transition to the FCC phase, the $C_{ss'}$ constants in figure 9 grow monotonically without any signs of softening. This reflects the smooth variation of $n(\varepsilon)$ and $C^b_{ss'}$ in the BCC phase for $U \leqslant U_{c1}$ (figure 2). At the same time, the decrease of U in the FCC phase from $U \simeq 0.5$ to $U \leqslant U_{c1}$ causes a sharp drop of C' down to large negative values at $U \simeq 0.3$. Figures 2 and 13 show that this is a typical 'band' drop of C' connected with the passage of ε_F through the $n(\varepsilon)$ peak corresponding to the point X in the BZ. Thus, according to our calculations, the phase transition from the BCC phase of Cs under pressure is an example of a transition without pre-martensitic anomalies, while in an inverse transition from the FCC phase such anomalies should be clearly pronounced. It seems very interesting to verify experimentally such a peculiar asymmetry of the pre-martensitic phenomena.

On further increase of the FCC Cs compression, the isostructural 's–d' phase transition with a large jump of the volume $\Delta U = 0.04$, is observed at $U_{c2} = 0.56$ [29]. The appreciable softening of the C_{44} constant as U approaches U_{c2} (see figure 9) is a non-trivial prediction of our calculations. This softening of C_{44} is also a conventional band effect connected with ε_F creeping over the d peak in $n(\varepsilon)$, and thus this effect may be not too sensitive to the approximations used in the calculation.

We did not succeed in calculating the band structure and $C^b_{ss'}$ in Cs for still greater $U \geqslant 0.55$–0.60 relevant to the region after the s–d transition. Under these U (as well as at $U \geqslant 0.40$ in Ba or $U \geqslant 0.55$ in Sr and Ca), a noticeable overlapping of the considered valence electronic states with the core ones begins, both in conventional space and in energy. Thus, the usual approximations of the LMTO-ASA method used become inapplicable. However, for $U \leqslant 0.55$ the methods employed seem to be sufficiently reliable. Therefore, the softening of the C_{44} constants predicted by us at large $U \geqslant 0.50$ in cubic phases of akaline-earth metals and Cs (as well as possibly of K and Rb) can be a band effect general for all these phases, which reflects the tendency towards phase transitions to complex structures, e.g. Cs–IV.

5. Concluding remarks

Let us make remarks about the accuracy of the methods used to estimate $C_{ss'}$. They are based on the electronic structure calculations by the LMTO-ASA method, the precision of which is apparently high enough; see, e.g. [23, 26]. For the metals considered this is also illustrated by the above-mentioned agreement of our results for $n(\varepsilon)$ and ε_{nk} with those obtained earlier by different methods. The main errors in the calculations are evidently due to the neglect of the $C_{ss'}^{m}$ contributions to equation (5) and the approximation (6) with $A = 5/3$ for $C_{ss'}^{es}$, the accuracy of which is generally speaking not clear.

The results in figures 5–9 make one infer that our calculations usually somewhat underestimate $C_{ss'}$ and overestimate the band effects of their softening, though at $U = 0$, as mentioned, the errors are not large. Using Cs as an example, we have remarked that one of the reasons for underestimating $C_{ss'}$ may be the fact that in expression (6) for $C_{ss'}^{es}$, instead of the nominal metal valence Z, its 'electrostatic' value Z_0 should be substituted, which is determined by the actual value of the electron density Z_0/Ω in the interstitial space [19]. For simplicity, above we have allowed for the correction induced by the replacement of Z with Z_0 in equation (6) only for Cs (where it is particularly large) and disregarded the possible dependence of Z_0 on U. The substitution of Z_0 for Z in the alkaline-earth metals also somewhat increases $C_{ss'}^{es}$ (at $U = 0$ by 15–20%). This may somewhat improve the accuracy of the total $C_{ss'}$ description in these metals as well.

The use of the 'electrostatic' Z_0 value in equation (6) instead of the nominal Z may turn out to be particularly important for transition metals. To verify that, we have applied the estimate (6) to the case of the C' constant in Pd and Au, which have been treated in detail by Christensen [15]. His thorough and consistent calculations yielded the C'_{es} value of 36 GPa in both Pd and Au. At the same time, the relation (6) with $A = 5/3$ and the Z_0 and Ω values from [19] (Z_0(Pd) = 3.19, Z_0(Au) = 3.43, Ω_{Pd} = 99.3 au, Ω_{Au} = 113.3 au) yields 36.2 and 35.1 GPa for C'_{es} in Pd and Au, respectively. Such a close agreement may, of course, be accidental. However, it may also corroborate the above considerations about the 'electrostatic' meaning of $Z = Z_0$ in equation (6), as well as the possibility of using the estimate (6) also for other metals.

Let us now discuss the physical results of the work. Of most interest seems to be the relation between certain changes of the band structure and those of the shear constants, in particular their pre-martensitic softening near structural phase transition points. In all the metals considered (except the BCC Cs) the proximity of the compression U to the transition point U_c is accompanied by the 'band' softening of one or both shear constants, and usually this softening is connected with the fact that the Fermi level ε_F approaches the peak or another maximum of the density of states $n(\varepsilon)$. A similar connection was noted in the literature for a number of other systems, e.g. Ni–Ti alloys and A-15 type systems. At the same time, the absence of such singularities in the band-structure evidently results in the absence of the mentioned anomalies, which was illustrated above by the BCC Cs case. In this connection one may assume that the closeness of ε_F to the peak or another singular $n(\varepsilon)$ point (or the absence of such closeness) precisely determines the presence (or absence) of lattice softening near the structural phase transition points in metals and alloys. The theoretical and experimental verification of this hypothesis seems important for microscopic understanding of the nature of pre-martensitic phenomena, which until now have been discussed mainly phenomenologically (see e.g. [8, 9]).

The results of this work also illustrate the fact that the ε_F proximity to the singular $n(\varepsilon)$ points causes the greatest lability, i.e. the variability of the $C_{ss'}$ constants on changing

external parameters. Earlier this was remarked for models of the rigid-band type in [1–3, 17, 18].

Finally, the concrete predictions of anomalies in the $C_{ss'}(U)$ dependences for the considered metals also seem significant. The most interesting seem to be the sharp softening of the C' constant on both sides (in pressure p) of the FCC–BCC transition point in Sr and Ca, the presence of a similar C' softening in Cs with decreasing p in the FCC phase and its absence with rising p in the BCC phase, as well as the presence (under high compressions $U > 0.45$) of appreciable softening of the C_{44} constant in BCC Sr and FCC Cs. The experimental verification of these predictions seems to be important for the development of adequate ideas about the influence of electronic structure on the properties of metals.

Acknowledgment

The authors are grateful to N E Zein for numerous discussions and for his interest in this work.

References

[1] Ashkenazi J, Dacorogna M, Peter M, Talmor Y, Walker E and Steinemann S 1978 *Phys. Rev.* B **18** 4120
[2] Bujard P, Sanjines R, Walker E, Ashkenazi J and Peter M 1981 *J. Phys. F: Met. Phys.* **11** 775
[3] Ohta Y and Shimizu M 1983 *J. Phys. F: Met. Phys.* **13** 761
[4] Voronov F F and Stalgorova O V 1978 *Fiz. Tverd. Tela* **20** 452
[5] Goncharova V A, Il'ina G G and Voronov F F 1982 *Fiz. Tverd. Tela* **24** 1849
[6] Voronov F F, Gromnitskaya E L and Stalgorova O V 1987 *Fiz. Metall. Metalloved.* **64** 1084
[7] Vaks V G, Katsnelson M I, Koreshkov V G, Likhtenstein A I, Parfenov O E, Skok V F, Sukhoparov V A, Trefilov A V and Chernyshov A A 1989 *J. Phys.: Condens. Matter* **1** 5319
[8] Kondrat'ev V V and Pushin V G 1985 *Fiz. Metall. Metalloved.* **60** 629
[9] Verlinden B and Delaey L 1988 *Acta Metall.* **36** 1771
[10] Andersen O K 1975 *Phys. Rev.* B **12** 3060
[11] Moruzzi V L, Janak J F and Williams A R 1978 *Calculated Electronic Properties of Metals* (New York: Pergamon)
[12] Jansen H J and Freeman A J 1984 *Phys. Rev.* B **30** 561
[13] Lam P K, Chou M Y and Cohen M L 1984 *J. Phys. C: Solid State Phys.* **17** 2065
[14] Maysenhölder W, Louie S G and Cohen M L 1983 *Phys. Rev.* B **31** 1817
[15] Christensen N E 1984 *Solid State Commun.* **49** 701
[16] Chen J, Boyer L L, Krakauer H and Mehl M J 1988 *Phys. Rev.* B **37** 3295
[17] Vaks V G and Trefilov A V 1983 *Pis. Zh. Eksp. Teor. Fiz.* **38** 373
[18] Vaks V G and Trefilov A V 1988 *J. Phys. F: Met. Phys.* **18** 213
[19] Dacorogna M, Ashkenazi J and Peter M 1982 *Phys. Rev.* B **26** 1527, 5975
[20] Olijnyk H and Holzapfel W B 1984 *Phys. Lett.* A **100** 191
[21] Skriver H L 1985 *Phys. Rev.* B **31** 1909
[22] Chen Y, Ho K-M and Harmon B N 1988 *Phys. Rev.* B **37** 283
[23] Andersen O K 1984 *The Electron Structure of Complex Systems* ed W Temmerman and P Phariseau (New York: Plenum)
[24] Hedin L and Lundquist J 1971 *J. Phys. C: Solid State Phys.* **4** 2064
[25] Pettifor D G 1977 *J. Phys. F: Met. Phys.* **13** 613
[26] Mackintosh A R and Andersen O K 1979 *Electrons at the Fermi Surface* ed M Springfold (Cambridge: Cambridge University Press) p 149
[27] Zein N E 1984 *Fiz. Tverd. Tela* **28** 3028
[28] Mahan G D 1981 *Many-Particle Physics* (New York: Plenum) p 399
[29] Boehler R and Ross M 1984 *Phys. Rev.* B **29** 3673
[30] Vaks V G and Trefilov A V 1977 *Fiz. Tverd. Tela* **19** 244
[31] Vaks V G, Samolyuk G D and Trefilov A V 1988 *Phys. Lett.* A **127** 37
[32] Vaks V G, Zarochentsev E V, Kravchuk S P and Safronov V P 1978 *J. Phys. F: Met. Phys.* **8** 725
[33] Anisimov V I, Vaks V G and Susloparov G A 1990 *Fiz. Tverd. Tela* **32** (3) 918